sciendo

Int. J. of Applied Mechanics and Engineering, 2020, vol.25, No.3, pp.1-16
DOI: 10.2478/ijame-2020-0031

ANALYSIS OF STRUCTURAL CONCRETE BAR MEMBERS BASED ON SECANT STIFFNESS METHODS

AYAD AL-RUMAITHI, AQEEL T. FADHIL* and BAN FADHIL SALMAN
Department of Civil Engineering, University of Baghdad
Baghdad, IRAQ
E-mails: ayad.a@coeng.uobaghdad.edu.iq; aqeel.fadhil@uobaghdad.edu.iq;
ban.fadhil@coeng.uobaghdad.edu.iq

In this paper, the behavior of structural concrete linear bar members was studied using numerical model implemented in a computer program written in MATLAB. The numerical model is based on the modified version of the procedure developed by Oukaili. The model is based on real stress-strain diagrams of concrete and steel and their secant modulus of elasticity at different loading stages. The behavior presented by normal force-axial strain and bending moment-curvature relationships is studied by calculating the secant sectional stiffness of the member. Based on secant methods, this methodology can be easily implemented using an iterative procedure to solve non-linear equations. A comparison between numerical and experimental data, illustrated through the strain profiles, stress distribution, normal force-axial strain, and moment-curvature relationships, shows that the numerical model has good numerical accuracy and is capable of predicting the behavior of structural concrete members with different partially prestressing ratios at serviceability and ultimate loading stages.

Key words: secant stiffness, numerical model, prestressed, structural concrete.

1. Introduction

Prestressed concrete beams have been widely used in structural engineering especially in the field of bridge engineering due to the need for long span structures. It is worth mentioning that fully prestressed concrete has better mechanical properties than ordinary reinforced concrete, but it has less ductility, making it less alarming because of smaller deflection and cracking [1]. Partially prestressed concrete beams came as an intermediate solution between fully prestressed concrete and ordinary reinforced concrete, making it a desirable choice for concrete designs [2].

An analysis of prestressed concrete members can be performed based on either cross-sectional concept methods or by discrete methods. The finite element method, which is considered one of the powerful discrete methods, has been used to accurately predict the behavior of ordinary and prestressed concrete members [3, 4, 5]. A simpler approach can be adopted by studying the member cross-sections rather than the full member. Several researchers have investigated the strength of structural concrete cross-sections, including Oukaili [6, 7], Kawakami *et al.* [8, 9] and Rodríguez-Gutiérrez *et al.* [10]. Oukaili presented an terative methodology of analysis based on the secant sectional stiffness rather than the tangential sectional stiffness. Secant stiffness methods can be easily implemented and have more numerical stability than tangential stiffness methods. The secant sectional stiffness is calculated by area integration of secant modulus of elasticity of the materials in the cross-section. In Oukaili's works [6, 7], the constitutive relationships of materials and the secant moduli of elasticity were adopted from the model suggested by Karpenko *et al.* [11], which is capable of showing full non-linear behavior of concrete in compression and tension and also for steel. Oukaili's methodology has been implemented in a computer program written in

* To whom correspondence should be addressed

FORTRAN language [6] and applied after modifications to solve different structural analyzing problems (i.e., strength, cracking and deformability) including ordinary reinforced concrete, partially and fully prestressed concrete members and GFRP bar reinforced concrete beams [12, 13].

The objective of this study is to investigate the behavior of structural concrete linear bar members, using the methodology presented by Oukaili [7], and taking into consideration the decreasing effect of the prestressing force due to the progress of the nonlinearity of this steel with the progress of the applied load. To achieve this goal, the computer FORTRAN program which was written by Oukaili [6] should be modified and re-written in MATLAB. The modified program will use the same numerical model based on the methodology presented by Oukaili [7]. The adopted numerical model will be compared to the available experimental data mentioned in Oukaili [6].

2. Numerical model

The numerical model consists of two parts: the stress-strain model and the force vector-strain vector model. Karpenko model [11] was used to simulate the stress-strain diagrams of concrete and steel and to determine their secant modulus of elasticity.

The force vector-strain vector model finds the relationship between the section forces vector (i.e., axial force and biaxial moments) with the strain vector (axial strain and curvature in both directions). It is based on the secant sectional stiffness. The methodology requires integration of the resisting forces of all the involved cross-sectional components based on their secant modulus of elasticity of the participating materials in the cross-section, and it also requires iterations to solve the non-linear equations in order to find the components of the strain vector.

2.1. Stress-strain model

The model of Karpenko *et al.* [11] for concrete and steel is adopted in this study. The model takes the following form

$$\sigma_m = \varepsilon_m E_m v_m \tag{2.1}$$

in which $(E_m v_m)$ represents the secant modulus of elasticity at the nonlinear portion of the stress-strain curve, while (v_m) equals (1) in the linear portion and less than (1) in the nonlinear portion of the stress-strain curve. Karpenko derived the following expression for (v_m) in the nonlinear portion

$$\begin{aligned} & v_m^2\left[1+\frac{e_{2m}\left(v_o-\hat{v}_m\right)^2\ \tilde{\varepsilon}_m^2}{\hat{v}_m^2\ \left(1-\tilde{\sigma}_{m,el}\right)^2}\right]-v_m\left[2\hat{v}_m-\frac{\tilde{\varepsilon}_m\left(v_o-\hat{v}_m\right)^2}{\hat{v}_m\left(1-\tilde{\sigma}_{m,el}\right)}\left(e_{1m}-\frac{2\ e_{2m}\ \tilde{\sigma}_{m,el}}{1-\widetilde{\sigma}_{m,el}}\right)\right]+ \\ & +\left[\hat{v}_m^2-\left(v_o-\hat{v}_m\right)^2\left(1+\frac{e_{1m}\ \tilde{\sigma}_{m,el}}{1-\tilde{\sigma}_{m,el}}-\frac{e_{2m}\ \tilde{\sigma}_{m,el}^2}{\left(1-\tilde{\sigma}_{m,el}\right)^2}\right)\right]=0 \end{aligned} \tag{2.2}$$

with

$$\hat{v}_m=\frac{\hat{\sigma}_m}{\left|\hat{\varepsilon}_m\right|\ E_m},\qquad \tilde{\varepsilon}_m=\left|\frac{\varepsilon_m}{\hat{\varepsilon}_m}\right|,\qquad \tilde{\sigma}_{m,el}=\left|\frac{\sigma_{m,\ el}}{\hat{\sigma}_m}\right|,\qquad e_{2m}=1-e_{1m} \tag{2.3}$$

where: m – the subscript assigns the type of material; $\hat{\sigma}_m$ – the ultimate strength of material; $\hat{\varepsilon}_m$ – the material strain corresponding to $\hat{\sigma}_m$; E_m – the initial modulus of elasticity; $\hat{v}_m$ – the value of v_m which

corresponds to the stress $\hat{\sigma}_m$; ε_m – the material strain level; $\sigma_{m,el}$ – the maximum elastic stress of the material; e_{1m}, e_{2m} – the actors depend on material type; v_o – the factor depending on the stress level.

The value (v_m) is calculated by finding the two roots of Eq.(2.2) and choosing the highest value of them. The factors e_{1m}, e_{2m} and v_o are explained in detail in Karpenko.

2.2. Force vector-strain vector model

The force vector-strain vector model, which was rewritten in MATLAB, was used to analyze structural concrete linear bar members. This method is based on the secant sectional stiffness. It is a modified version of the methodology presented by Oukaili [7]. The main difference involves that the modified version takes into account the reduction of prestressing force due to the nonlinearity of the behavior of this steel beyond the proportionality limit. This method requires the iterative process to solve non-linear equations. It is based on the following assumptions:

1) Strain distribution across the section is proportional to the distance from the global reference axes in accordance with Bernoulli-Navier's hypothesis "cross section shall remain plane after bending".
2) Shear and torsion stresses are ignored.
3) The analytical constitutive relationships of steel and concrete are considered to follow Karpenko model, where all stresses in concrete and steel are related to the secant modulus of elasticity.
4) A perfect bond exists between the concrete and the internal reinforcement, where the strain of the nonprestressed steel and the strain increment of the bonded prestressed steel due to the applied load are compatible with the strain of the concrete fiber which exists at their centers of gravity.
5) The concrete region is divided into a group of small bar elements having cross-sectional sizes related to the required accuracy conditions. Meanwhile, the steel bars, wires, or strands act as a system of linear elements exposed to axial compression or tension.

Using Karpenko model and applying equilibrium conditions to the member cross-section, the following equations can be written

$$N = \sum_{i=1}^{r} \varepsilon_{ci} E_c v_{ci} A_{ci} + \sum_{j=1}^{p} \varepsilon_{sj} E_s v_{sj} A_{sj}, \tag{2.4}$$

$$M_x = \sum_{i=1}^{r} \varepsilon_{ci} E_c v_{ci} A_{ci} y_{ci} + \sum_{j=1}^{p} \varepsilon_{sj} E_s v_{sj} A_{sj} y_{sj}, \tag{2.5}$$

$$M_y = \sum_{i=1}^{r} \varepsilon_{ci} E_c v_{ci} A_{ci} x_{ci} + \sum_{j=1}^{p} \varepsilon_{sj} E_s v_{sj} A_{sj} x_{sj} \tag{2.6}$$

where: N, M_x, M_y – the axial force, the moment around x - axis and moment around the y - axis, respectively; i, j – subscripts assign concrete and steel elements; $\varepsilon_{ci}, \varepsilon_{sj}$ – the strain of concrete and steel elements, respectively; E_c, E_s – the modulus of elasticity of concrete and steel, respectively; v_{ci}, v_{sj} – the secant modulus of elasticity factors of concrete and steel which are functions of ε_{ci}, ε_{sj} per Karpenko model; x_{ci}, y_{ci} – the distance from the area center gravity of the concrete bar element to the arbitrary (reference) global axes, respectively; x_{sj}, y_{sj} – the distance from the center of the steel bar element to the arbitrary global axes, respectively; A_{ci}, A_{sj} – the cross-sectional area of the concrete bar element and the

steel bar element, respectively; r, p – the number of concrete bar elements and steel bar elements in the general cross-section, respectively.

The strain values depend on the strain vectors as shown in the following equation

$$\varepsilon_{ci} = \varepsilon_o + K_x y_{ci} + K_y x_{ci}, \tag{2.7}$$

$$\varepsilon_{sj} = \varepsilon_o + K_x y_{sj} + K_y x_{sj} \tag{2.8}$$

where: ε_o – the axial strain; K_x – the curvature of the member longitudinal axis in the OYZ plane; K_y – the curvature of the member longitudinal axis in the OYX plane.

Substitute Eq.(2.7) and Eq.(2.8) in Eq.(2.4), Eq.(2.5), and Eq.(2.6) to get

$$N = \sum_{i=1}^{r}\left(\varepsilon_o + K_x y_{ci} + K_y x_{ci}\right) E_c v_c A_{ci} + \sum_{j=1}^{p}\left(\varepsilon_o + K_x y_{sj} + K_y x_{sj}\right) E_s v_s A_{sj}, \tag{2.9}$$

$$M_x = \sum_{i=1}^{r}\left(\varepsilon_o + K_x y_{ci} + K_y x_{ci}\right) E_c v_c A_{ci} y_{ci} + \sum_{j=1}^{p}\left(\varepsilon_o + K_x y_{sj} + K_y x_{sj}\right) E_s v_s A_{sj} y_{sj}, \tag{2.10}$$

$$M_y = \sum_{i=1}^{r}\left(\varepsilon_o + K_x y_{ci} + K_y x_{ci}\right) E_c v_c A_{ci} x_{ci} + \sum_{i=1}^{p}\left(\varepsilon_o + K_x y_{sj} + K_y x_{sj}\right) E_s v_s A_{si} x_{sj}. \tag{2.11}$$

Decompose the above equations and arrange them in a matrix form between forces vector $|F|$, strain vector $|\bar{\varepsilon}|$ and secant stiffness matrix $[C]$ can be expressed as follows

$$|F| = [C]^* |\bar{\varepsilon}|. \tag{2.12}$$

This expression is detailed as follows

$$\begin{vmatrix} N \\ M_x \\ M_y \end{vmatrix} = \begin{bmatrix} C_{11} & C_{12} & C_{13} \\ C_{21} & C_{22} & C_{23} \\ C_{31} & C_{32} & C_{33} \end{bmatrix} \begin{vmatrix} \varepsilon_o \\ K_x \\ K_y \end{vmatrix} \tag{2.13}$$

where the elements of the secant stiffness matrix are shown below

$$C_{11} = \sum_{i=1}^{r} E_c v_{ci} A_{ci} + \sum_{j=1}^{p} E_s v_{sj} A_{sj}, \tag{2.14}$$

$$C_{12} = C_{21} = \sum_{i=1}^{r} E_c v_{ci} A_{ci} y_{ci} + \sum_{j=1}^{p} E_s v_{sj} A_{sj} y_{sj}, \tag{2.15}$$

$$C_{13} = C_{31} = \sum_{i=1}^{r} E_c v_{ci} A_{ci} x_{ci} + \sum_{j=1}^{p} E_s v_{sj} A_{sj} x_{sj}, \tag{2.16}$$

$$C_{22} = \sum_{i=1}^{r} E_c v_{ci} A_{ci} y_{ci}^2 + \sum_{j=1}^{p} E_s v_{sj} A_{sj} y_{sj}^2 , \tag{2.17}$$

$$C_{33} = \sum_{i=1}^{r} E_c v_{ci} A_{ci} x_{ci}^2 + \sum_{j=1}^{p} E_s v_{sj} A_{sj} x_{sj}^2 , \tag{2.18}$$

$$C_{23} = C_{32} = \sum_{i=1}^{r} E_c v_{ci} A_{ci} x_{ci} y_{ci} + \sum_{j=1}^{p} E_s v_{sj} A_{sj} x_{sj} y_{sj} . \tag{2.19}$$

For prestressed concrete sections, an additional term ε_{psj} should be added to Eq.(2.8) to include the initial strain of prestressed steel strands as shown below

$$\varepsilon_{sj} = \varepsilon_o + K_x y_{sj} + K_y x_{sj} + \varepsilon_{psj} . \tag{2.20}$$

Substitute Eq.(2.20) in Eq.(2.4), Eq.(2.5), and Eq.(2.6) to get

$$N = \sum_{i=1}^{r} \left(\varepsilon_o + K_x y_{ci} + K_y x_{ci} \right) E_c v_c A_{ci} + \sum_{j=1}^{p} \left(\varepsilon_o + K_x y_{sj} + K_y x_{sj} + \varepsilon_{psj} \right) E_s v_s A_{sj} , \tag{2.21}$$

$$M_x = \sum_{i=1}^{r} \left(\varepsilon_o + K_x y_{ci} + K_y x_{ci} \right) E_c v_c A_{ci} y_{ci} + \sum_{j=1}^{p} \left(\varepsilon_o + K_x y_{sj} + K_y x_{sj} + \varepsilon_{psj} \right) E_s v_s A_{sj} y_{sj} , \tag{2.22}$$

$$M_y = \sum_{i=1}^{r} \left(\varepsilon_o + K_x y_{ci} + K_y x_{ci} \right) E_c v_c A_{ci} x_{ci} + \sum_{j=1}^{p} \left(\varepsilon_o + K_x y_{sj} + K_y x_{sj} + \varepsilon_{psj} \right) E_s v_s A_{sj} x_{sj} . \tag{2.23}$$

After decomposing and rearranging, we get terms independent of the strain vector. Equation (2.12) shall be modified into

$$\left| F \right| = \left[C \right] * \left| \bar{\varepsilon} \right| + \left| F_{ps} \right| \tag{2.24}$$

where

$$\left| F_{ps} \right| = \begin{vmatrix} N_{ps} \\ M_{x_{ps}} \\ M_{y_{ps}} \end{vmatrix} \tag{2.25}$$

and

$$N_{ps} = \sum_{j=1}^{p} E_s v_{sj} \varepsilon_{psj} A_{sj} , \tag{2.26}$$

$$M_{x_{ps}} = \sum_{j=1}^{p} E_s v_{sj} \varepsilon_{psj} A_{sj} y_{sj} , \tag{2.27}$$

$$M_{y_{ps}} = \sum_{j=1}^{p} E_s v_{sj} \varepsilon_{psj} A_{sj} x_{sj} \,. \tag{2.28}$$

Since $\left|F_{ps}\right|$ components depend on v_{sj} values, the value remains constant at the linear range and then starts to decrease when the steel strand enters the inelastic range. This term takes into account the decreasing effect of the axial force and moment of prestressing tendons due to the progress of the nonlinearity of this steel with the progress of the applied load. Figure 1 shows the change of N_{ps} of a single strand with its strain.

The matrix $[C]$ and vector $\left|F_{ps}\right|$ are functions of the strain vector. Accordingly, Eq.(2.24) can be rewritten in the following form

$$\left|\bar{\varepsilon}\right| = C\left(\left|\bar{\varepsilon}\right|\right)^{-1} * \left(\left|F\right| - \left| F_{ps}\left(\left|\bar{\varepsilon}\right|\right)\right| \right). \tag{2.29}$$

Equation (2.29) is a non-linear expression which requires an iterative solution. In the first iteration, the strain vector is assumed equal to the initial value which is usually zero. So, the stiffness matrix can be calculated easily. Equation (2.30) is used then to evaluate the strain vector resulted from the first iteration. For further iterations, the stiffness matrix will be updated according to the strain vector calculated from the previous iteration as shown below

$$\left|\bar{\varepsilon}\right|_k = C\left(\left|\bar{\varepsilon}\right|_{k-1}\right)^{-1} * \left(\left|F\right| - \left| F_{ps}\left(\left|\bar{\varepsilon}\right|_{k-1}\right)\right| \right) \tag{2.30}$$

where subscript (k) represents iteration number.

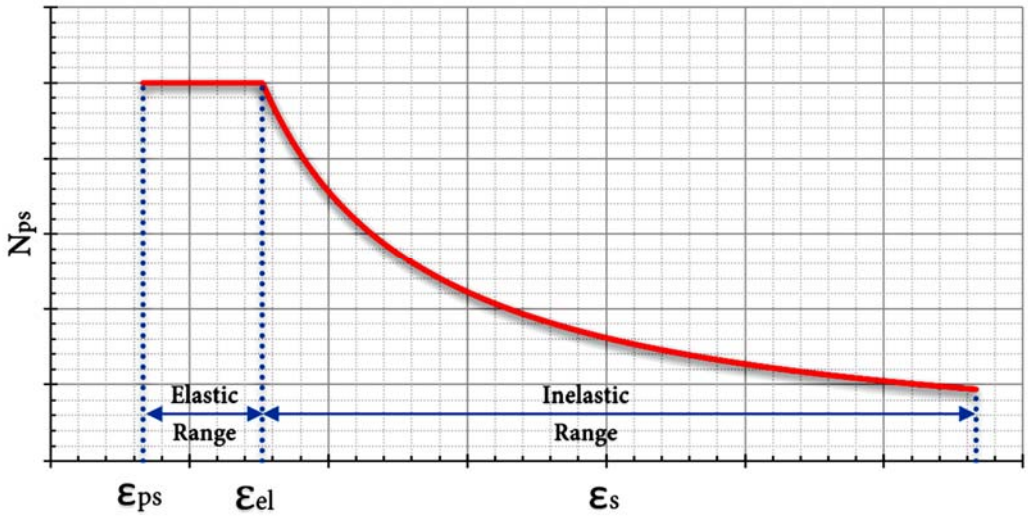

Fig.1. Variation of N_{ps} with strain for a single strand.

The procedure is repeated until the convergence of the strain vector satisfies the following condition

$$\left|\bar{\varepsilon}\right|_k - \left|\bar{\varepsilon}\right|_{k-1} < \delta \tag{2.31}$$

where (δ) represents the convergence limit for the strain vector which is usually a very small value. The flow chart of the iterative procedure is shown in Fig.2.

Since it is based on secant methods, this procedure can be easily implemented and can give good numerical accuracy and stability.

3. Verification of the numerical model

Four simply supported partially prestressed concrete beams were tested by Oukaili [9]. These beams were subjected to four-point bending up to failure using two concentrated loads at the middle third of the span. All beams are with rectangular cross-section with *3000 mm* clear span. Two types of reinforcement were implemented: nonprestressed and prestressed steel. Two beams have identical reinforcement as shown in Fig.3. Beams 3 and 4 have similar top reinforcement to Beam 1 and 2 but higher bottom reinforcement, higher prestressing forces and higher partially prestressing ratio. Strains were measured by installing strain gauges at midspan section across the depth. In order to ensure accuracy, three strain gauges were installed at the same level and the average of the three readings was considered. The failure midspan moments where *120 kN.m*, *120 kN.m*, *140 kN.m* and *145 kN.m* for Beams 1, 2, 3 and 4, respectively.

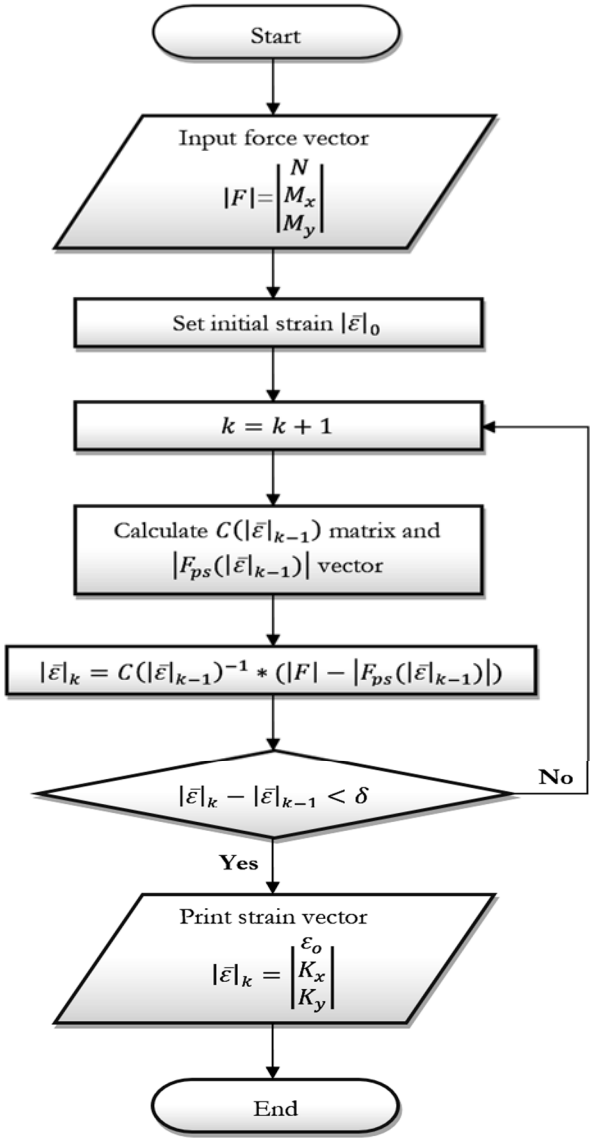

Fig.2. Flow chart of the iterative procedure.

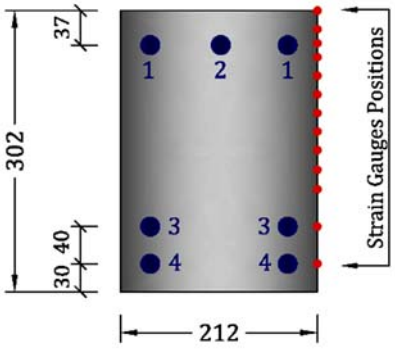

No.	Description
1	Ø10 bar
2	As=0.96 cm² Strand with σ_{ps}=623 MPa
3	As=0.96 cm² Strand with σ_{ps}=1027 MPa
4	As=0.96 cm² Strand with σ_{ps}=0 MPa

a) Beam 1

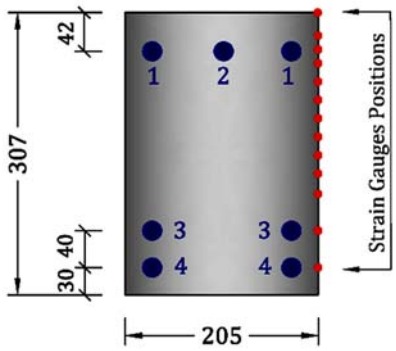

No.	Description
1	Ø10 bar
2	As=0.96 cm² Strand with σ_{ps}=623 MPa
3	As=0.96 cm² Strand with σ_{ps}=1027 MPa
4	As=0.96 cm² Strand with σ_{ps}=0 MPa

b) Beam 2

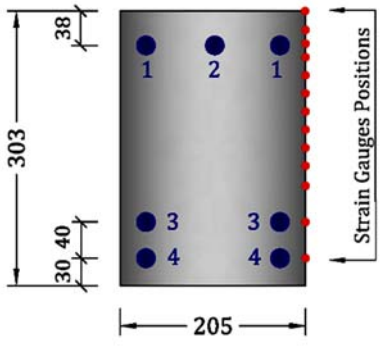

No.	Description
1	Ø10 bar
2	As=0.96 cm² Strand with σ_{ps}=623 MPa
3	As=1.40 cm² Strand with σ_{ps}=1109 MPa
4	Ø14 bar

c) Beam 3

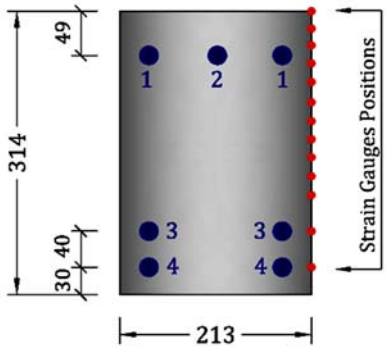

No.	Description
1	Ø10 bar
2	As=0.96 cm² Strand with σ_{ps}=623 MPa
3	As=1.40 cm² Strand with σ_{ps}=1109 MPa
4	Ø14 bar

d) Beam 4

Fig.3. Beam dimensions (mm) and reinforcement details of the specimens.

All materials which were used in the fabrication of the experimental beams were tested to determine their physical-mechanical properties. Table 1 shows the ultimate tensile strength, yield strength, modulus of elasticity and ultimate tensile strain of steel bars and strands. Also, Tab.2 shows the ultimate compressive strength, modulus of rupture, modulus of elasticity and ultimate compressive strain.

Table 1. Mechanical properties of steel bars and strands.

Steel Type	**Ultimate Tensile Strength, (MPa)**	**Yield Strength, (MPa)**	**Modulus of Elasticity, (GPa)**	**Ultimate Tensile Strain**
$\phi 10$ Bars	*620*	*420*	*200*	*0.2*
Strands ($A_s = 0.96\ cm^2$)	*1846.55*	*1437.85*	*165.35*	*0.06*
Strands ($A_s = 1.40\ cm^2$)	*1645*	*1293*	*178.65*	*0.0356*
$\phi 14$ Bars	*1199*	*998*	*191.40*	*0.0720*

Table 2. Concrete mechanical properties.

Concrete Type	Ultimate Compressive Strength, (MPa)	Modulus of Rupture, (MPa)	Modulus of Elasticity, (GPa)	Ultimate Compressive Strain
C50 (Beams 1 and 2)	*50.6*	*4.22*	*32.9*	*0.003*
C51 (Beams 3 and 4)	*51.9*	*4.33*	*35.75*	*0.003*

4. Comparison between numerical model and experimental data

Numerical stress-strain diagrams of steel and concrete were generated using Karpenko model based on the materials parameters in Tabs 1 and 2. Figure 4 shows the stress-strain curves of both materials. As shown, the model is capable of showing compressive hardening and softening, tension softening in concrete, hardening in steel and yield plateau in steel bars.

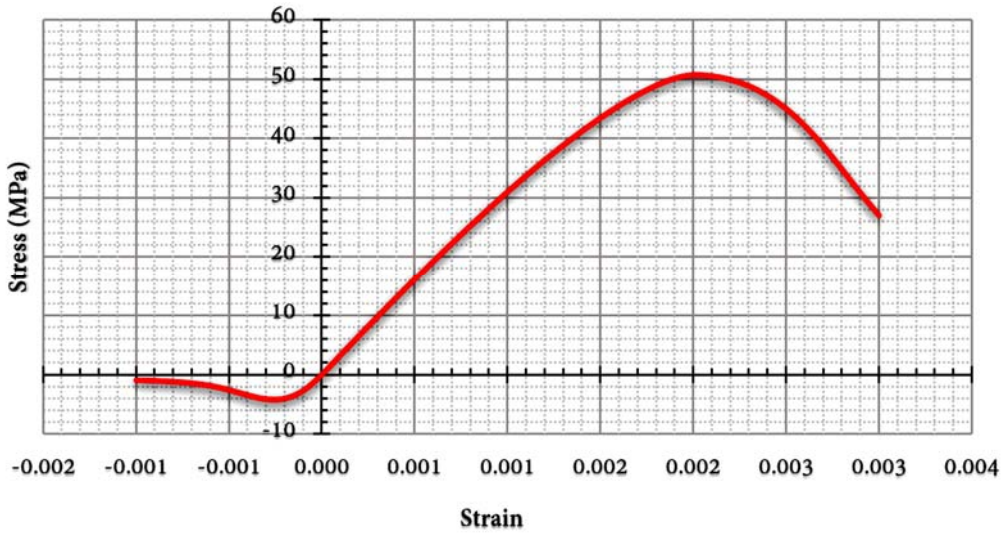

Fig.4.a. Stress-strain diagrams of concrete, steel bars and steel strands per Karpenko model: Stress-strain diagram of C50 concrete.

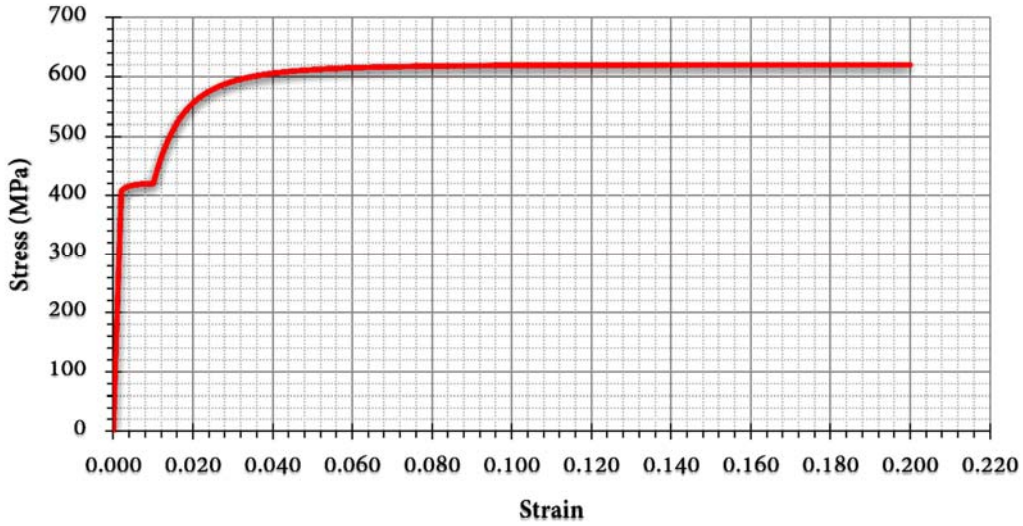

Fig.4.b. Stress-strain diagrams of concrete, steel bars and steel strands per Karpenko model: Stress-strain diagram of $\phi 10$ bar.

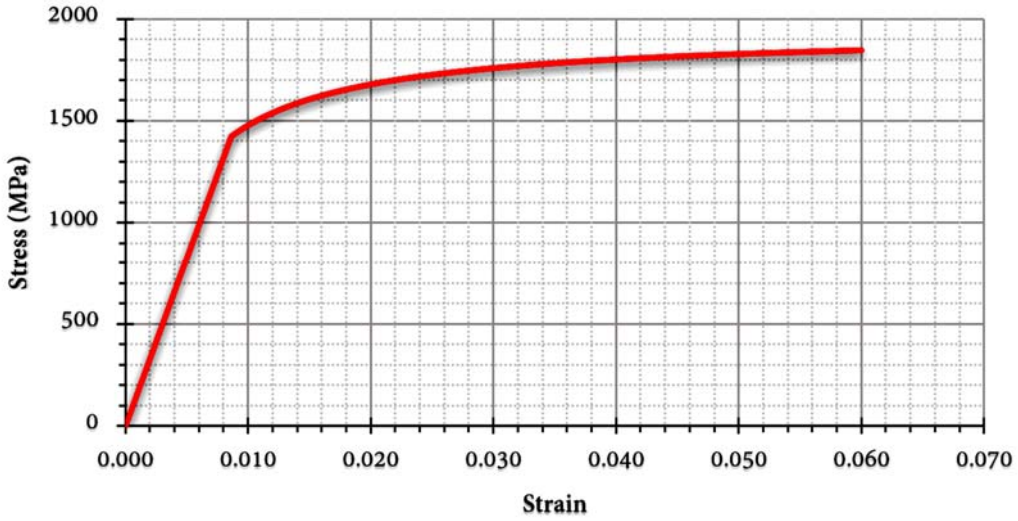

Fig.4.c Stress-strain diagrams of concrete, steel bars and steel strands per Karpenko model: Stress-strain diagram of steel strand with $A_s = 0.96\,cm^2$.

The beams cross-sections in Fig.3 were modeled using the method explained in Section 2.2. The beams models were subjected to different values of uniaxial bending moment at major direction (M_x) and compared to the corresponding experimental data. In Fig.5 and Fig.6, strain profiles are shown at two levels of loadings: $M_x = 30\,kNm$ (elastic range) and $M_x = 90\,kNm$ (inelastic range).

In Fig.5, the strain profiles are shown for the beams subjected to $M_x = 30\,kNm$. The dots represent experimental strain values at this loading stage subtracted from the initial strain value and will be called "strain increment". Solid lines represent first order regression of the strain increment values. The slope of this line with respect to the vertical line represents the curvature increment, which is the value of curvature at this loading stage subtracted from the initial curvature value and will be denoted as $\bar{K}_{x_{Exp}}$. The strain profile predicted by the model is shown by the dashed lines in the figure. The values of curvature predicted from the numerical model are also subtracted from the initial curvature of the model and denoted as $\bar{K}_{x_{Num}}$. The values of $\bar{K}_{x_{Exp}}$ and $\bar{K}_{x_{Num}}$ of the beams are shown in the figure. The values of experimental data and numerical results were compared and the discrepancy between $\bar{K}_{x_{Exp}}$ and $\bar{K}_{x_{Num}}$ values are *6.6*%, *21.4*%, *2.6*% and *20.7*% for beams 1, 2, 3 and 4, respectively. The average discrepancy for beam 1 and 2 is *14* % and for beams 3 and 4 is *10.7*%. The average value of the four beams is *12.4*%.

Figure 6 shows strain profiles for both experimental and numerical results at $M_x = 90$ *kNm*. For experimental results, the strain gauges located at a crack position at tension zone were excluded from the comparison due to inaccuracy. For this loading stage, the discrepancy between $\bar{K}_{x_{Exp}}$ and $\bar{K}_{x_{Num}}$ are *13.8*%, *25.5*%, *11*% and *1.7*% for beams 1, 2, 3 and 4, respectively. The average discrepancy for beams 1 and 2 is *19.7*% and for beams 3 and 4 is *6.4*%. The average value of the four beams is *13.1*%.

Figure 7 shows the moment-curvature relationship for the numerical model and experimental data subjected to incremental loading. As beams 1 and 2 have lower reinforcement and lower partially prestressing ratios than beams 3 and 4, the figures show that their moment-curvature behavior is governed by strand yielding (tension controlled). It shows also that they have higher curvature values than beams 3 and 4.

It can be seen from the figures that the proposed model seems to have a higher stiffness than the experimental model. This slight difference can be attributed to different reasons. This first reason could be

related to concrete cracking induced by the drying shrinkage in the experimental model which contributes to the reduction in the stiffness of the tested beams. The assumption of perfect bond between the concrete and the reinforcing steel and the absence of prestress losses and slip in the numerical model make it stiffer than the experimental model. Creep could be another factor that explains the discrepancy between the behavior of the tested beams and the numerical model [14-20].

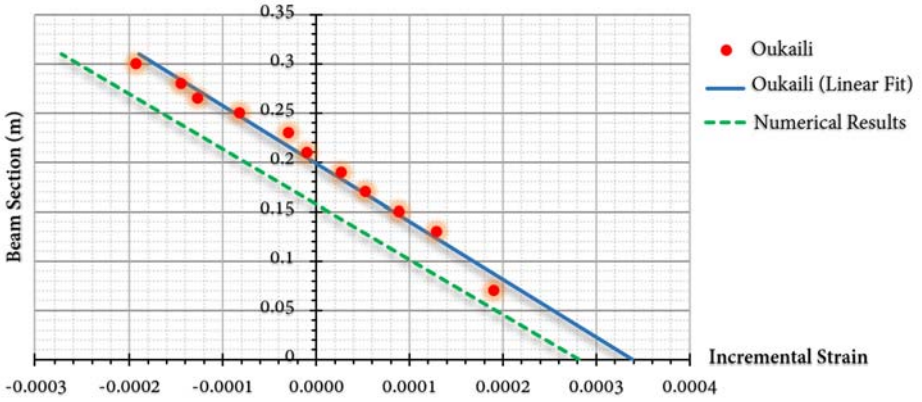

Fig.5.a. Strain profiles at $M_x = 30\ kNm$ (elastic range): Beam 1 $\left(\bar{K}_{x_{Exp}} = 0.0017 \frac{1}{m},\ \bar{K}_{x_{Num}} = 0.00182 \frac{1}{m} \right)$.

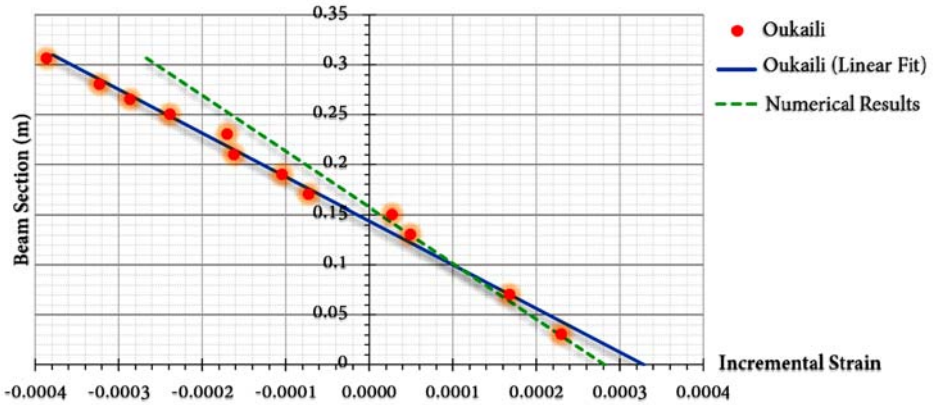

Fig.5.b. Strain profiles at $M_x = 30\ kNm$ (elastic range): Beam 2 $\left(\bar{K}_{x_{Exp}} = 0.00228 \frac{1}{m},\ \bar{K}_{x_{Num}} = 0.00179 \frac{1}{m} \right)$.

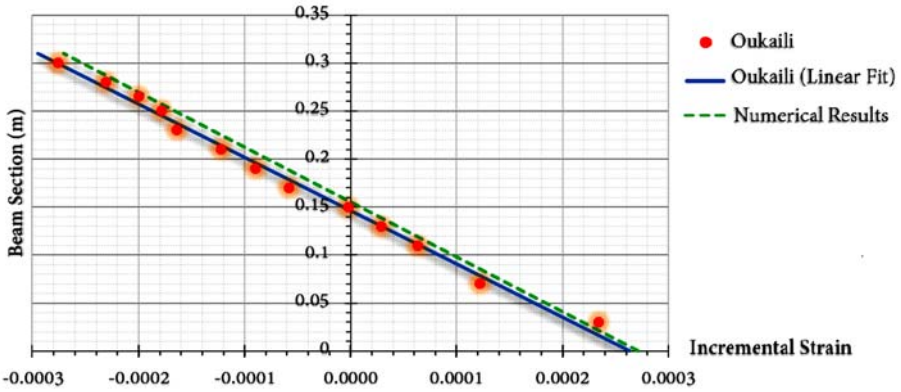

Fig.5.c Strain profiles at $M_x = 30\ kNm$ (elastic range): Beam 3 $\left(\bar{K}_{x_{Exp}} = 0.0018 \frac{1}{m},\ \bar{K}_{x_{Num}} = 0.00181 \frac{1}{m} \right)$

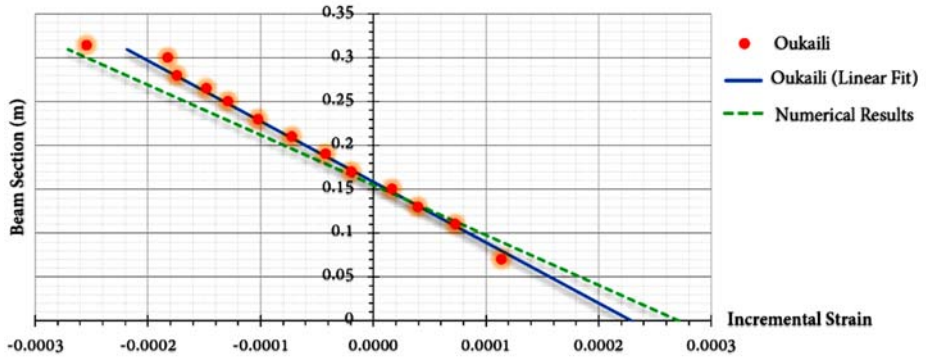

Fig.5.d. Strain profiles at $M_x = 30\ kNm$ (elastic range): Beam 4 $\left(\bar{K}_{x_{Exp}} = 0.00145\frac{1}{m},\ \bar{K}_{x_{Num}} = 0.00175\frac{1}{m} \right)$.

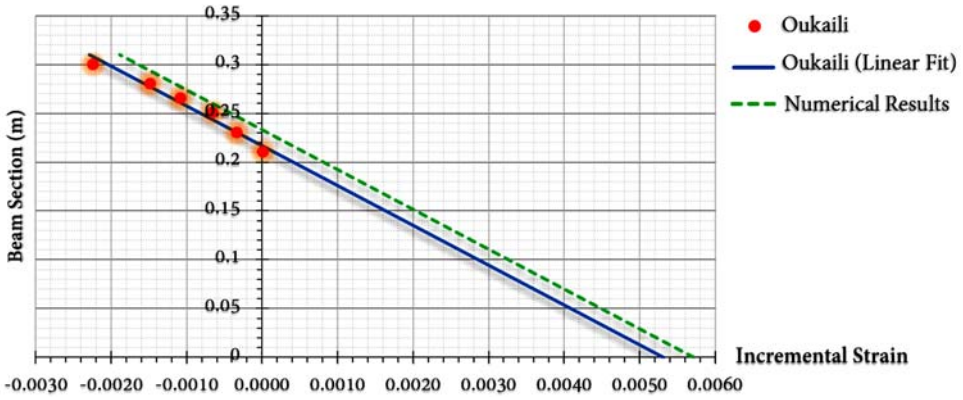

Fig.6.a. Strain profiles at $M_x = 90\ kNm$ (inelastic range): Beam 1 $\left(\bar{K}_{x_{Exp}} = 0.029\frac{1}{m},\ \bar{K}_{x_{Num}} = 0.0250\frac{1}{m} \right)$.

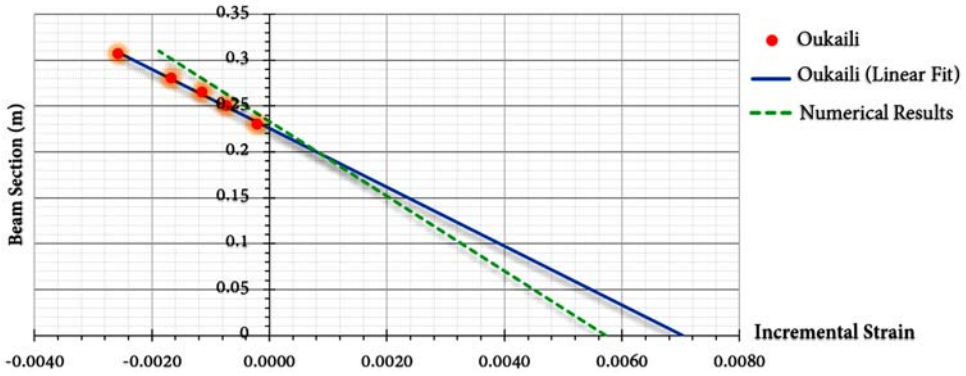

Fig.6.b Strain profiles at $M_x = 90\ kNm$ (inelastic range): Beam 2 $\left(\bar{K}_{x_{Exp}} = 0.033\frac{1}{m},\ \bar{K}_{x_{Num}} = 0.0246\frac{1}{m} \right)$.

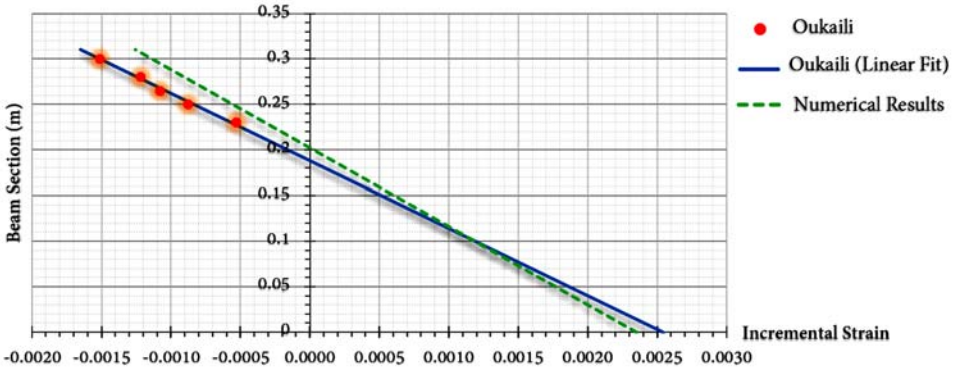

Fig.6.c. Strain profiles at $M_x = 90\ kNm$ (inelastic range): Beam 3 $\left(\bar{K}_{x_{Exp}} = 0.0136 \frac{1}{m},\ \bar{K}_{x_{Num}} = 0.0121 \frac{1}{m} \right)$.

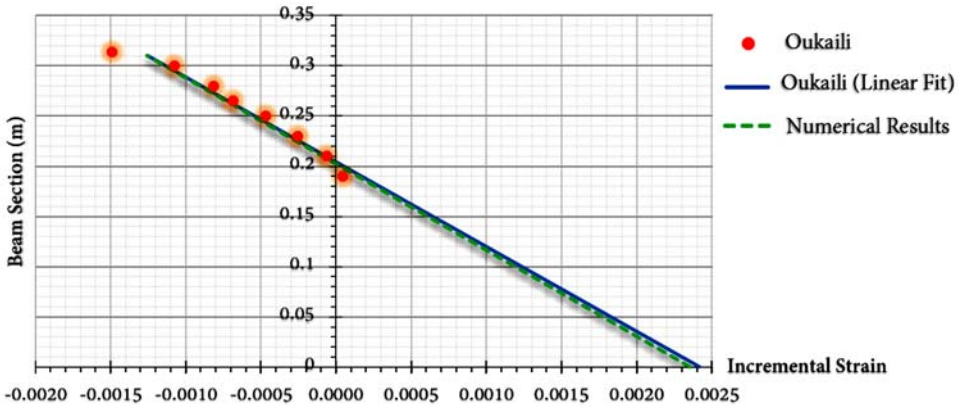

Fig.6.d. Strain profiles at $M_x = 90\ kNm$ (inelastic range): Beam 4 $\left(\bar{K}_{x_{Exp}} = 0.0119 \frac{1}{m},\ \bar{K}_{x_{Num}} = 0.0117 \frac{1}{m} \right)$.

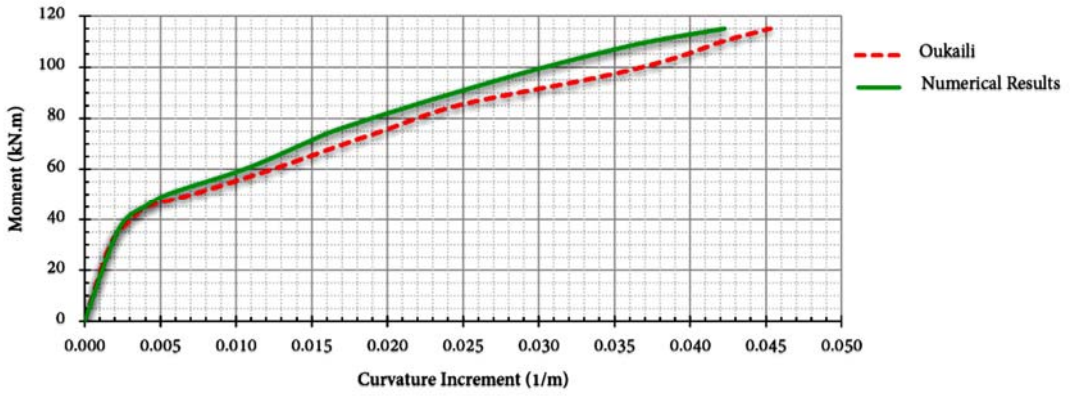

Fig.7.a. Moment-curvature diagrams: Beam 1.

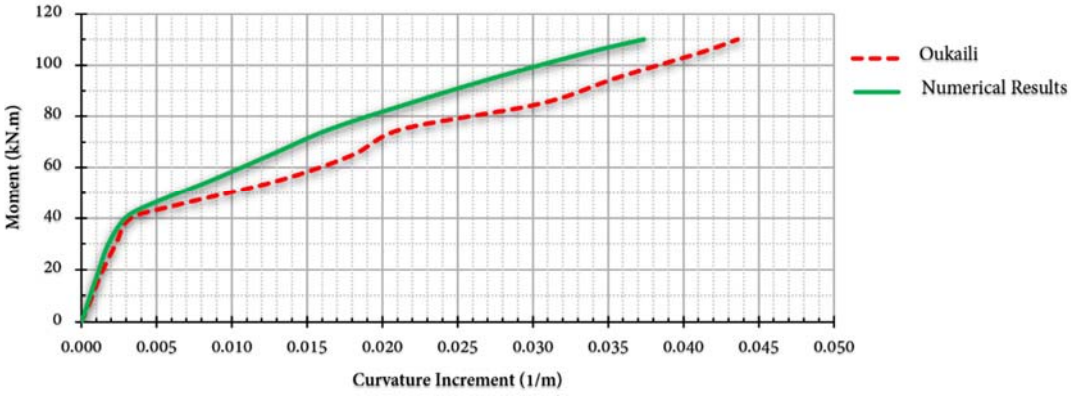

Fig.7.b. Moment-curvature diagrams: Beam 2.

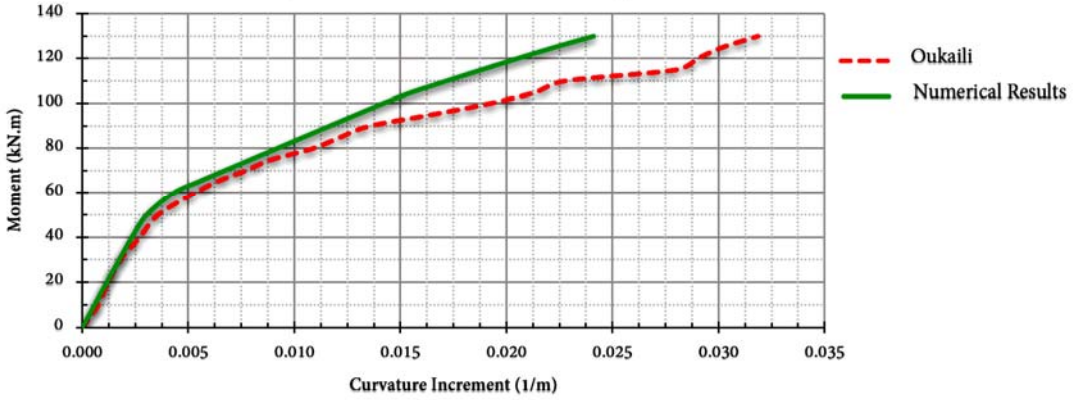

Fig.7.c. Moment-curvature diagrams: Beam 3.

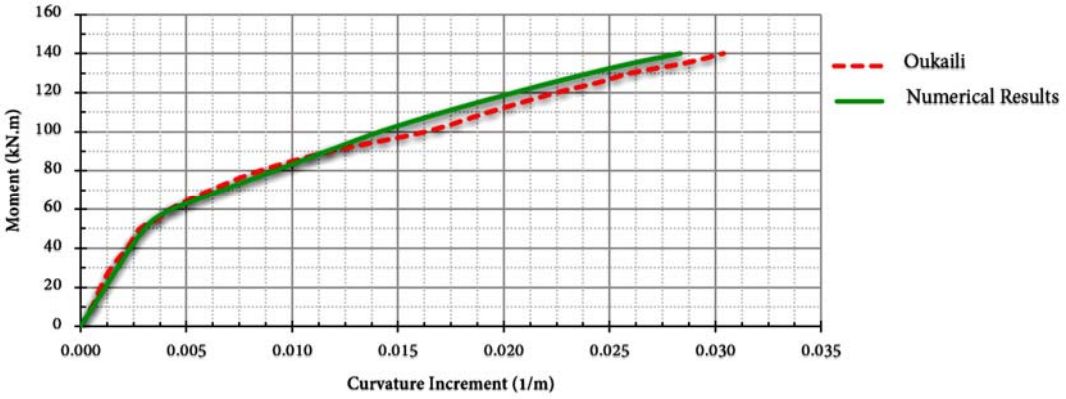

Fig.7.d. Moment-curvature diagrams: Beam 4.

5. Conclusion

In the current study, the behavior of partially prestressed concrete beams was studied using a computer program written in MATLAB. The model is based on real stress-strain diagrams of concrete and steel and their secant modulus of elasticity. The beam sections behavior presented by force vector-strain vector relationship is studied by calculating the secant sectional stiffness of the beams. The model requires an iterative procedure to solve non-linear equations. The numerical model is based on a modified version of the methodology presented by Oukaili [7]. The numerical model is compared with experimental data of loading four partially prestressed beams subjected to flexure. It was shown that the numerical model was

capable of predicting the performance of the prestressed concrete beams at different loading stages. Meanwhile, the model can deal with structural beams with different values of reinforcement and partially prestressing ratios.

Nomenclature

ε_m – material strain level
E_m – initial modulus of elasticity
v_m – secant modulus of elasticity factor
σ_m – material stress level
m – subscript assigns the type of material
$\hat{\sigma}_m$ – ultimate strength of material
$\hat{\varepsilon}_m$ – material strain corresponding to $\hat{\sigma}_m$
$\hat{v}_m$ – value of v_m which corresponds to the stress $\hat{\sigma}_m$
e_{1m}, e_{2m} – factors depending on material type
v_o – factor depending on the stress level
N, M_x, M_y – axial force, the moment around the x-axis and moment around the y-axis, respectively
i, j – subscripts assign concrete and steel elements, respectively
$\varepsilon_{ci}, \varepsilon_{sj}$ – strain of concrete and steel elements, respectively
E_c, E_s – modulus of elasticity of concrete and steel, respectively
v_{ci}, v_{sj} – secant modulus of elasticity factors of concrete and steel, respectively
x_{ci}, y_{ci} – distance from the area center gravity of the concrete bar element to the arbitrary (reference) global axes, respectively
x_{sj}, y_{sj} – distance from the center of the steel bar element to the arbitrary global axes, respectively
A_{ci}, A_{sj} – cross-sectional area of the concrete bar element and the steel bar element, respectively
r, p – number of concrete bar elements and steel bar elements in the general cross-section, respectively
ε_o – axial strain
K_x – curvature of the member longitudinal axis in the OYZ plane
K_y – curvature of the member longitudinal axis in the OYX plane
$|F|$ – forces vector
$|\overline{\varepsilon}|$ – strain vector
$[C]$ – secant stiffness matrix
ε_{psj} – prestrain of the steel element
$|F_{ps}|$ – prestressed forces vector
$N_{ps}, M_{x_{ps}}, M_{y_{ps}}$ – prestressed axial force, the moment around the*x*-axis and moment around the *y*-axis, respectively
k – subscript represents iteration number
δ – convergence limit for the strain vector
$\overline{K}_{x_{Exp}}$ – experimental value of curvature at loading stage subtracted from the initial curvature value
$\overline{K}_{x_{Num}}$ – numerical value of curvature at loading stage subtracted from the initial curvature value

References

[1] Zandi Y., Akgun Y. and Durmus A. (2012): *Investigating the use of high-performance concrete in partially prestressed beams and optimization of partially prestressed ratio*. – Indian Journal of Science and Technology, vol.5, No.7, pp.2991-2996.

[2] Abdelrahman A.A. (1995): *Serviceability of concrete beams prestressed by fiber reinforced plastic tendons*. – Ph.D. Thesis, Manitoba Univ., Manitoba.

[3] Chen W., Hao H. and Chen S. (2015): *Numerical analysis of prestressed reinforced concrete beam subjected to blast loading.* – Materials and Design (1980-2015), vol.65, pp.662-674.

[4] Yapar O., Basu P.K. and Nordendale N. (2015): *Accurate finite element modeling of pretensioned prestressed concrete beams.* – Engineering Structures, vol.100, pp.163-178.

[5] Wolanski A.J. (2004): *Flexural behavior of reinforced and prestressed concrete beams using finite element analysis*. – Ph.D. Thesis.

[6] Oukaili N.K. (1991): *Strength of partially prestressed concrete elements with mixed reinforcement by highly strength strands and steel bars*. – Ph.D. Thesis, Moscow Civil Engineering Univ., Moscow, (in Russian).

[7] Oukaili N.K. (1997): *Moment capacity and strength of reinforced concrete members using stress-strain diagrams of concrete and steel.* – Journal of King Saud University, vol.10, pp.23-44.

[8] Kawakami M. and Ghali A. (1996): *Time-dependent stresses in prestressed concrete sections of general shape*. – PCI Journal, vol.41, No.3.

[9] Kawakami M. and Ghali A. (1996): *Cracking, ultimate strength, and deformations of prestressed concrete sections of general shape.* – PCI Journal, vol.41, No.4, pp.114-122.

[10] Rodríguez-Gutiérrez J.A. and Aristizábal-Ochoa J.D. (2000): *Partially and fully prestressed concrete sections under biaxial bending and axial load.* – Structural Journal, vol.97, No.4, pp.553-563.

[11] Karpenko N.I., Mukhamediev T.A. and Petrov A.N. (1986): *The initial and transformed stress-strain diagrams of steel and concrete.* – Special Publication in: Stress-Strain Condition for Reinforced Concrete Construction, Reinforced Concrete Research Center, Moscow, pp.7-25, (in Russian).

[12] Oukaili N.K. and Al-Hawwassi I.F. (2010): *Short term deflection of ordinary, partially prestressed and GFRP bars reinforced concrete beams.*– Journal of Engineering, vol.16, No.1, pp.4631-4652.

[13] Oukaili N.K. and Buniya M.K. (2013): *Serviceability performance of externally prestressed steel-concrete composite girders.*– Journal of Engineering, vol.19, No.6, pp.734-751.

[14] Gilbert R.I. (2013): *Time-dependent stiffness of cracked reinforced and composite concrete slabs*. – Procedia Engineering, vol.57, pp.19-34.

[15] Gilbert R.I. and Ranzi G. (2011): *Time-dependent deformation.* In: Time-Dependent Behaviour of Concrete Structures (1st Ed.) – Milton, England: Spon Press.

[16] Gilbert R.I., Bradford M.A., Gholamhoseini A. and Chang Z-T. (2012): *Effects of shrinkage on the long-term stresses and deformations of composite concrete slabs.* – Engineering Structures, vol.40, pp.9-19.

[17] Kaklauskas G. and Gribni V. (2011): *Eliminating shrinkage effect from moment-curvature and tension-stiffening relationships of reinforced concrete members*. – Journal of Structural Engineering (ASCE), vol.137, No.12, pp.1460-1469.

[18] Kaklauskas G., Gribniak V., Bacinskas D. and Vainiunas P. (2009): *Shrinkage influence on tension-stiffening relationships in concrete members.* – Engineering Structures, vol.31, No.6, pp.1305-1312.

[19] Kaklauskas G. and Ghaboussi G. (2001): *Stress-strain relations for cracked tensile concrete from RC beam tests.* – Journal of Structural Engineering (ASCE), vol.12, No.1, pp.64-73.

[20] Bischoff P.H. (2001): *Effects of shrinkage on tension stiffening and cracking in reinforced concrete.* – Canadian Journal of Civil Engineering, vol.28, No.3, pp.363-374.

Received: October 15, 2019

Revised: Mai 5, 2020